NONLINEAR HYDBRID SLIDING MODE CONTROL OF AN ELECTROHYDRAULIC ACTIVE SUSPENSION

Shaer, Bassel[a], Kenné, Jean-Pierre[b], Kaddissi, Claude[c], Polotski, Vladimir[d]

[a] [b] [c] [d] Mechanical Engineering Department, Laboratory of Integrated Production Technologies, Université du Québec, École de Technologie Supérieure, 1100, Notre Dame Street West, Montreal QC H3C 1K3, Canada
Tel. +1-514-396-8800, FAX +1-514-396 8530,

[a]bassel.shaer.1@ens.etsmtl.ca , [b]jean-pierre.kenne@etsmtl.ca, [c]claude.kaddissi@etsmtl.ca,
[d]Vladimir.Polotski@etsmtl.ca

ABSTRACT
This paper introduces the multi-objective control and modeling of a nonlinear electrohydraulic active suspension. By using a hybrid control algorithm, the objective of tracking a desired force and position was optimized to reach a satisfactory performance. When designing such a controller, a compromise needed to be made between the ride quality and the road handling. The controller structure was built in three stages, in which the sliding mode approach was used to produce the proper control signal that satisfies the requested control objective. The simulation results for position control showed that the controller was able to isolate the passengers from the road irregularities, but with significant transmitted force. In order to reduce the transmitted force to passengers, a force sliding mode controller was developed, but the passengers' vertical motion was unsatisfactory. A hybrid control algorithm was developed to track a desired vertical position and to reduce the transmitted force to the passengers at the same time. The two controllers have been added by two low pass filters with a variable gain to give priority to the force controller to react in the case of high transmitted force. These filters delay the control signals in order to prevent the singularity in simulation. The simulation results show that hybrid sliding mode control achieved a very good compromise between the two objectives without involving complex control strategies.

Keywords: hybrid control, sliding mode, position control, force control, active suspension system

1. INTRODUCTION
Recent research in electrohydraulic systems (EHS), which is very popular due to its high force-to-weight ratio and fast response, concentrates on the control of position and force separately. Most applications in industry, like robots and production machines, require accuracy in position control with some considerations to produced force.

Some applications require force tracking, but with some position limitations. From this perspective, researchers concentrated on the position control (Choi, Tafazoli et al 1998, Avila et al 2004, Indrawanto et al 2011, Rahmat et al 2011).

Many control strategies have been used to track the position of an electrohydraulic system. One of the most interesting theories is the variable structure control, or sliding mode control (SMC). The sliding mode control is known for its robustness against uncertainties, and is applicable to linear systems as well as nonlinear systems (Hashemipour et al 2009). Since the position control often leads to an undesired force magnitude in an electrohydraulic active suspension system, it is necessary to control the force magnitude by different control strategies. In (Chantranuwathana and Peng 1999), the problem of force tracking has been divided into two parts: the first part is considered as a main loop for producing the desired force by an LQ controller, and the second part is an adaptive robust controller to track the desired force under uncertainties in the system parameters.

In electrohydraulic systems, system performance at high frequencies can be deteriorated due to unmodeled dynamics. This was improved in the work of (Chantranuwathana and Peng 2000), who considered the effect of unmodeled dynamics of servo valve and the delay of the applied control signal in their algorithm. On the other side, estimation of parameters with feedback linearization has a significant effect on the position control. In (Angue-Mintsa et al 2011), an adaptive feedback linearization is applied in order to feedback estimated parameters to improve the control operation. The principle of linking two loops has been used by (Sam and Hudha 2006). An outer loop was used to calculate the force reference and an inner loop was used to ensure a small tracking error. A similar concept was used in (Shi and Liu 2011), where a double loop in auto disturbance rejection control is designed to ensure position control and

force control at the same time. As mentioned previously, when the attention was more focused on position control, the transmitted force was not acceptable. Therefore, the researchers started to express the problem differently, as in (Nguyen et al 2000), where a hybrid force/position control with sliding mode was proposed. The experimental results that were obtained showed good performance, but the desired force was chosen as a classical function of the position error by means of constant gains. This means that, if the tracking position error is a little high, the desired force will exceed the permitted limit. This is clear in the performance: they have a high tracking force error with position errors measuring many millimeters. Therefore, the position should be tracked by a robust controller rather than by a direct relation between force error and position error. A more complicated design was used by (Priyandoko et al 2009): four loops to accomplish hybrid control of position and force by applying a novel skyhook and adaptive neuro-active force control technique. They used a neural network with an adaptive algorithm to approximate the mass estimation and inverse dynamic of the actuator.

The technique produced good results for force tracking, but the position error was still high. In addition, the nonlinearity in the actuator was not modeled when designing the force controller. Another concept for controlling position and force was accomplished by (Assadsangabi et al 2009) using two references as the ideal skyhook model and ground skyhook model, with the condition of having knowledge of road perturbations. The two control signals were added linearly to form a final control signal. The performance was good in terms of achieving its objectives, but controlling both the position and acceleration of two masses was considerably weak. Trying to accomplish good acceleration/position tracking by controlling the movement of two masses is useless because of the high nonlinearity in the pressure dynamic equation.

In addition, the damping coefficient error of the selected references was not compensated, which yields to degradation in the performance.

This paper is organized as follows: the first section introduces the problem and describes the state of the art. The second section presents the modeling of the electrohydraulic active suspension system. The third section describes the position SMC controller. The fourth section shows the force SMC controller. Section 5 is dedicated to the main contribution of this paper, namely the hybrid force-position controller. A comparison between a classical PID and a hybrid SMC controller is presented in section 6. The last section presents a conclusion and a recap of our work.

2. ELECTROHYDRAULIC ACTIVE SUSPENSION MODELING

Figure 1 shows a quarter-car model of an electrohydraulic active suspension. The control cylinder is placed between the car mass and the tire mass in order to isolate the car body from road irregularities transmitted via the car tire.
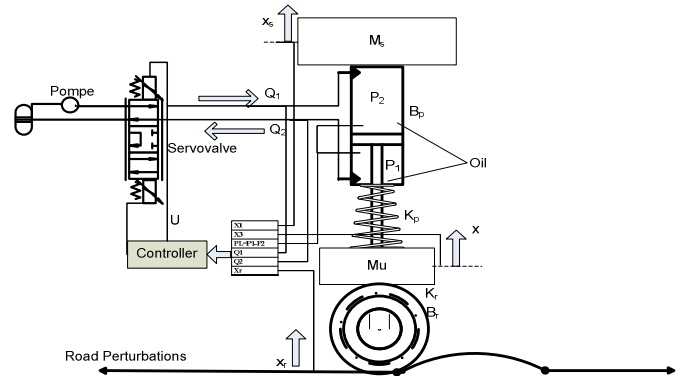

Figure 1: Active Suspension Bench

The active suspension mathematical model is derived from the mathematical model of an electrohydraulic system added to passive suspension.

The flow rate from and to the servo valve through the valve orifices, assuming symmetric and matched orifices with a small leakage, is given by (Merritt 1967):

$$Q_1 = Q_2 = C_d \; x_v \sqrt{\frac{P_S - \text{sign}(x_v)*P_L}{\rho}} \qquad (1)$$

The sign function, which expresses the change of the fluid flow direction, can be replaced by a differentiable function for numerical simulations, as suggested in (Kaddissi et al 2009). The compressibility equation that represents the load pressure dynamics is as follows:

$$\dot{P}_L = \frac{2\beta}{V_0}\left\{ C_d \; x_v \sqrt{\frac{P_s - P_L*sigm(x_v)}{\rho}} - L*P_L - A(\dot{x}_s - \dot{x}) \right\} \; (2)$$

The sigm function is defined as:

$$sigm(x_v) = \frac{1 - e^{-a\,x_v}}{1 + e^{-a\,x_v}}$$

We therefore have:

$$sigm(ax) = \begin{cases} 1 & if\ ax \to \infty \\ 0 & if\ ax \to 0 \\ -1 & if\ ax \to -\infty \end{cases}$$

and $\dfrac{d(sigm(a\,x_v))}{dt} = \dfrac{2a e^{-a\,x_v}}{\left(1 + e^{-a\,x_v}\right)^2}$

We now proceed to identify the car dynamics, using Newton's second law:

$$M_s \dot{x}_s = -k_p(x_s - x) - B_p(\dot{x}_s - \dot{x}) + A P_L \qquad (3)$$

$$M_u \dot{x} = k_p(x_s - x) + B_p(\dot{x}_s - \dot{x}) - k_r(x - x_r) - B_r(\dot{x} - \dot{x}_r) - A P_L \qquad (4)$$

Rewriting equations (2), (3) and (4) in terms of chosen variables $x_i : i = 1 \ldots 6$, we obtain a model as in (Kaddissi et al 2009). We propose another change of variables in order to include the suspension deflection, which is the difference between the car body position and the tire position. The control objective is to prevent this variable from hitting the imposed limits. The new state variables are:

$$y_1 = x_1, \ y_2 = x_2, \ y_3 = x_1 - x_3, \ y_4 = x_2 - x_4, \ y_5 = x_5,$$

$$y_6 = x_6$$

The model can be rewritten as follows:

$$\begin{cases} \dot{y}_1 = y_2 \\ \dot{y}_2 = -a_0 y_3 - b_0 y_4 + a_1 y_5 \\ \dot{y}_3 = y_4 \\ \dot{y}_4 = -A_1 y_3 - A_2 y_4 + A_3 y_5 + b_1 \dot{y}_r + h_1 y_r \\ \dot{y}_5 = \dfrac{J_1}{f(.)}\left(-A y_4 - L y_5 + C_d y_6 g(.)\right) \\ \dot{y}_6 = \dfrac{1}{\tau}\left(-y_6 + k u\right) \end{cases} \qquad (5)$$

Where:

$$A_1 = a_0 + d_0, \ A_2 = b_0 + d_1$$

$$A_3 = C_{10} + a_1, \ A_4 = J_1 * A$$

$$A_5 = J_1 * L, \ A_6 = J_1 * C_d$$

$$f(.) = V_0^2 - A^2 y_3^2$$

$$g(.) = \sqrt{\dfrac{P_s - sigm(y_6) y_5}{\rho}}$$

3. POSITION TRACKING CONTROL

The sliding mode is a nonlinear control strategy in which there is an invariant set that attracts every trajectory at the phase plan. Therefore, it is determined that S = 0 is a positive invariant set to attract the error trajectories. The control problem then reduces to (i) driving the system to this surface and (ii) ensuring that the system remains on this surface. We will calculate the command with the original coefficient of the system model. We first choose the surface S as:

$$S = c_1 y_1 + c_2 \dot{y}_1 + c_3 \ddot{y}_1 + c_4 \dddot{y}_1 \qquad (6)$$

We then calculate the derivative of y_1 (7) to use it in equation (6)

$$\begin{cases} \dot{y}_1 = y_2 \\ \ddot{y}_1 = \dot{y}_2 = -a_0 y_3 - b_0 y_4 + a_1 y_5 \\ \dddot{y}_1 = \ddot{y}_2 = -a_0 \dot{y}_3 - b_0 \dot{y}_4 + a_1 \dot{y}_5 \\ \quad = -a_0 y_4 - b_0(-A_1 y_3 - A_2 y_4 + A_3 y_5 + b_1 \dot{y}_r + h_1 y_r) \\ \quad + a_1(J_1(-A y_4 - L y_5 + C_d y_6 g(.))) \\ \quad = -b_0 A_1 y_3 - (a_0 - b_0 A_2 + a_1 J_1 A) y_4 + (-A_3 b_0 - a_1 L J_1) y_5 \\ \quad + a_1 C_d J_1 g(.) y_6 - b_0 b_1 \dot{y}_r - b_0 h_1 y_r \end{cases} \qquad (7)$$

Replacing (7) in (6) yields:

$$\begin{cases} S = c_1 y_1 + c_2 y_2 + (-a_0 c_3 + c_3 b_0 A_1) y_3 \\ -(c_4 a_0 + c_3 b_0 - c_4 b_0 A_2 + c_4 a_1 J_1 A_2) y_4 \\ -(A_3 b_0 c_4 - c_3 a_1 - c_4 a_1 J_1 L) y_5 \\ + c_4 a_1 C_d J_1 g(.) y_6 - c_4 b_0 b_1 \dot{y}_r \\ - c_4 b_0 h_1 y_r \end{cases} \qquad (8)$$

Now we take the derivative of S to realize the reaching condition (Fallaha et al 2011):

$$\dot{S} = -K_{sw} * \text{sign}(S) \qquad (9)$$

$$\begin{cases} \dot{S} = c_1 y_2 + c_2 \dot{y}_2 + (-a_0 c_3 + c_3 b_0 A_1) \dot{y}_3 \\ -(c_4 a_0 + c_3 b_0 - c_4 b_0 A_2 + c_4 a_1 J_1 A_2) \dot{y}_4 \\ -(A_3 b_0 c_4 - c_3 a_1 - c_4 a_1 J_1 L) \dot{y}_5 \\ + c_4 a_1 C_d J_1 g(.) \dot{y}_6 + c_4 a_1 C_d J_1 \dot{g}(.) y_6 \\ - c_4 b_0 b_1 \ddot{y}_r - c_4 b_0 h_1 \dot{y}_r \\ \quad = -K_{sw} * \text{sign}(S) \end{cases} \qquad (10)$$

We calculate the derivative of $g(.)$ and replace it in equation (10):

$$\begin{cases} \dot{g}(.) = \dfrac{1}{\sqrt{\rho}} * \dfrac{-[sig\dot{m}(y_6) * y_5 + sigm(y_6) \dot{y}_5]}{2\sqrt{P_s - sigm(y_6) y_5}} \\ \quad = \dfrac{1}{\sqrt{\rho}} * \dfrac{-\left[\dfrac{2a_2 e^{-a y_6}}{(1 + e^{-a y_6})^2} * y_5 + sigm(y_6) \dot{y}_5\right]}{2\sqrt{P_s - sigm(y_6) y_5}} \end{cases} \qquad (11)$$

To simplify the obtained expression, we choose:

$$\begin{cases} A_{41} = -c_4 a_0 + c_3 b_0 - c_4 b_0 A_2 + c_4 a_1 J_1 A \\ A_{42} = A_3 b_0 c_4 - c_3 a_1 - c_4 a_1 J_1 L \end{cases} \qquad (13)$$

We replace equation (13) in (12) to obtain:

$$
\left\{
\begin{array}{l}
\dot{S} = c_1 y_2 + \left[-c_2 a_0 + A_1 * A_{41} \right] y_3 \\
+ \left[-b_0 c_2 - a_0 c_3 + b_0 c_4 A_1 + A_1 * A_{41} + J_1 A_1 A \right] y_4 \\
+ \left[-c_2 a_1 - A_3 A_{41} + L A_{42} J_1 \right] y_5 - \dfrac{c_4 a_1 C_d J_1 g(.)}{\tau} y_6 \\
+ c_4 a_1 C_d J_1 \dot{g}(.) y_6 - A_{42} h_1 y_r - A_{42} \dot{b}_1 y_r \\
- c_4 b_0 b_1 \ddot{y}_r - c_4 b_0 h_1 \ddot{y}_r + \dfrac{c_4 a_1 C_d J_1 g(.) K}{\tau} U_{P_{SMC}} \\
= -K_{sw} * \text{sign}(S)
\end{array}
\right\} \quad (14)
$$

We extract the control signal $U_{P_{SMC}}$ to become:

$$
\left\{
\begin{array}{l}
U_{P_{SMC}} = \dfrac{\tau}{c_4 a_1 C_d J_1 g(.) K} * \\
\left[
\begin{array}{l}
-c_1 y_2 - \left[-c_2 a_0 + A_1 * A_{41} \right] y_3 \\
- \left[-b_0 c_2 - a_0 c_3 + b_0 c_4 A_1 + A_1 * A_{41} + J_1 A_1 A \right] y_4 \\
- \left[-c_2 a_1 - A_3 A_{41} + L A_{41} J_1 \right] y_5 + \dfrac{c_4 a_1 C_d J_1 g(.)}{\tau} y_6 \\
- c_4 a_1 C_d J_1 \dot{g}(.) y_6 + A_{42} h_1 y_r + A_{42} \dot{b}_1 y_r \\
+ c_4 b_0 b_1 \ddot{y}_r + c_4 b_0 h_1 \ddot{y}_r - K_{sw} * \text{sign}(S)
\end{array}
\right]
\end{array}
\right\} \quad (15)
$$

Therefore, the total control signal for the position control is:

$$ U_{P_{SMC}} = U_{P_{equ}} + U_{P_{sw}} \quad (16) $$

We can write $\dot{S}$ in the following form:

$$ \dot{S} = h(y) + O(y) U_{P_{sw}} \quad (17) $$

Suppose that $h(y), O(y)$ satisfies the inequality for some known function $\rho(y)$:

$$ \frac{h(y)}{O(y)} \leq \rho(y) \quad \forall \quad y \in R^2 \quad (18) $$

Where: $O(y) \geq O_0 \geq 0$

To prove the convergence of the sliding mode, we consider the derivative of the distance of the point from the sliding mode:

$$
\left\{
\begin{array}{l}
V = \dfrac{1}{2} S^2 \\
\dot{V} = S * \dot{S} = S * (h(y) + o(y) * U_{P_{smc}}) \\
\leq O(y) * |S| * \rho(y) + O(y) * S * U_{P_{smc}}
\end{array}
\right\} \quad (19)
$$

Taking:

$$ U_{P_{smc}} = -\beta(y) * \text{sgn}(S) \quad (20) $$

$\beta(y) \geq \rho(y) + \beta_0$ Where $\beta_0 > 0$,

$$
\text{sgn}(S) = \left\{
\begin{array}{ll}
1 & \text{if } S > 0 \\
0 & \text{if } S = 0 \\
-1 & \text{if } S < 0
\end{array}
\right\}
$$

This yields:

$$
\left\{
\begin{array}{l}
\dot{V} = O(y) |S| \rho(y) \\
- O(y) S (\rho(y) + \beta_0) \text{sign}(S) \\
= -O(y) \beta_0 |S| \leq -O_0 \beta_0 |S|
\end{array}
\right\} \quad (21)
$$

Therefore, the trajectory reaches the manifold $S = 0$ in finite time, and once on the manifold, it cannot leave it, as seen from the inequality $\dot{V} \leq -O_0 \beta_0 |S|$.

3.1. Position SMC control results:

We built our mathematical model in Matlab. The simulation was done with a small sampling time (0.0001 sec). In Figure 2, the perturbation signal is 10 cm, and the passenger seat position is deviated to 3 cm. This shows that the SMC controller exhibits a good performance. However, the force transmitted to the passengers is approximately 3400 N, which is too high (Figure 3). The control signal is well shaped, with no significant chattering.
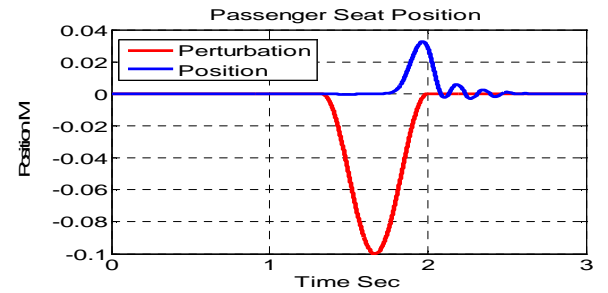

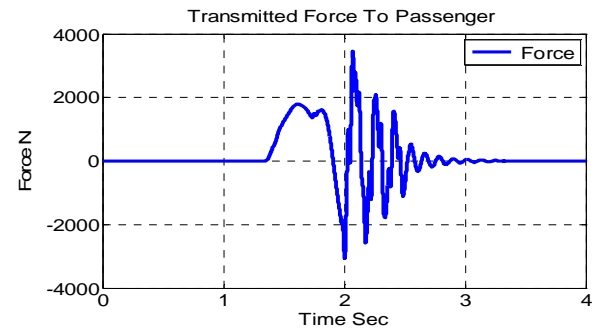Figure 2: Sprung Mass Position.
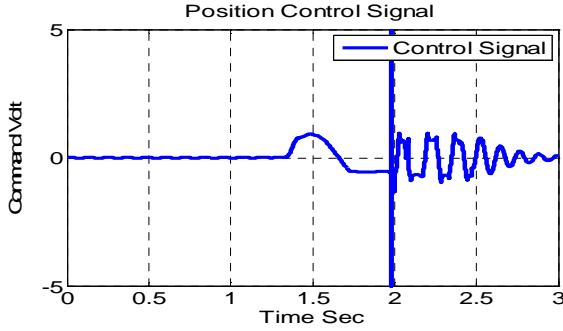

Figure 3: Force Transmitted To Passenger.

Figure 4: Control Signal

4. TRANSMITTED FORCE CONTROL

The force tracking is also accomplished by using the sliding mode controller. The surface of SMC is chosen as:

$$S = C_1(F - F_{des}) = C_1 A(y_5 - y_{5des}) \qquad (22)$$

The desired force has been chosen as follows (Sohl and Bobrow 1999):

$$F_{des} = M_v * ACC_{des} - K_v \left(\dot{y}_1 - \dot{y}_{1des} \right) - K_p \left(y_1 - y_{des} \right) \qquad (23)$$

Where: $F_{des} = A * y_{5des}$, this equation is derived from the car dynamics equations. When the error tracking position is zero, we will have $F_{des} = M_v * ACC_{des}$. This equation means that, when we track a desired position, the force being generated represents the desired force to be tracked.
We derive S as mentioned above in equation (9) to obtain the following control signal:

$$\begin{cases} \dot{S} = C_1 A(\dot{y}_5 - \dot{y}_{5des}) \\ = C_1 A \left[\dfrac{J_1}{f(.)} (-Ay_4 - Ly_5 + C_d y_6 g(.)) - y_{5des} \right] \\ = -K_{sw} * \text{sign}(S) \end{cases} \qquad (24)$$

From equation (5), we have $\dot{y}_6 = \frac{1}{\tau} \left(-y_6 + k\, U_{Fsmc} \right)$

This yields:

$$y_6 = -\tau \dot{y}_6 + k\, U_{Fsmc} \qquad (25)$$

Replacing (20) in (19), we obtain:

$$\dot{S} = C_1 A \left[\dfrac{J_1}{f(.)} (-Ay_4 - Ly_5 + C_d g(.)) \\ *(-\tau \dot{y}_6 + k U_{Fsmc})) - y_{5des} \right]$$

$$= \dfrac{C_1 A J_1}{f(.)} (-Ay_4 - Ly_5 - C_d g(.) \tau \dot{y}_6) \qquad (26)$$

$$+ C_d g(.) k U_{Fsmc}) - C_1 A y_{5des}$$

$$= -K_{sw} * \text{sign}(S)$$

Therefore, the equivalent control can be written as:

$$U_{fequ} = -\dfrac{\dfrac{C_1 A J_1}{f(.)} (-Ay_4 - Ly_5 - C_d g(.) \tau \dot{y}_6) - C_1 A y_{5des}}{\dfrac{C_1 A J_1 C_d g(.) k}{f(.)}}$$

$$(27)$$

The switching control:

$$U_{fsw} = -\dfrac{f(.)}{C_1 A J_1 C_d g(.) k} * k_{sw} * \text{sgn}(S) \qquad (28)$$

The total control signal for force tracking $U_{F_{SMC}}$:

$$U_{F_{SMC}} = U_{fequ} + U_{fsw} \qquad (29)$$

In simulation, the force controller demonstrated a significant force reduction, and the amplitude of the force transmitted to the passenger was reduced to 1200 N (Figure 5). In comparison with the position controller, the passenger force is reduced by 64%, which is a good index of controller efficiency. In terms of the position of the passenger's seat, there is no significant improvement or deterioration (Figure 6). Figure 7 shows the corresponding control signal with a maximum of 0.5 volt.
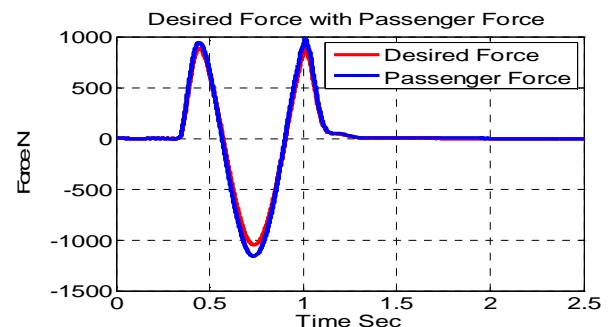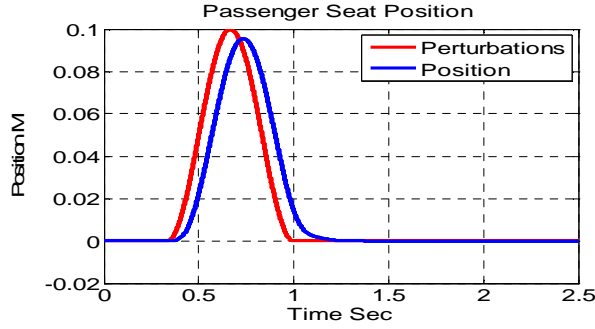

Figure 5: Force Tracking with SMC.
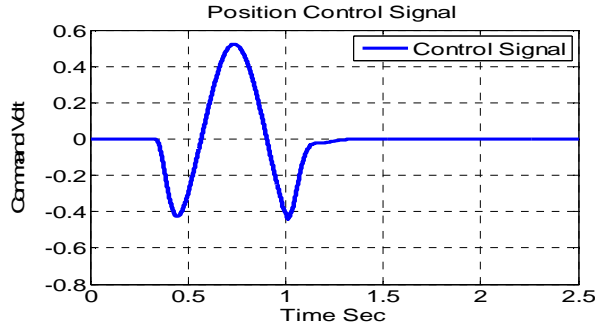
Figure 6: Sprung Mass Position

Figure 7: Control Signal

5. HYBRID POSITION-FORCE CONTROL

This section describes the main contribution of this paper, which proposes the hybrid multi-objective controller that is designed to achieve both a reduction of the passengers' vertical motion and a reduction of the force transmitted to them at the same time. The control signal is given by:

$$U_{tot} = \frac{\alpha_1}{s + \alpha_2} U_{P_{SMC}} + K1 \frac{\alpha_3}{s + \alpha_4} U_{F_{SMC}} \qquad (30)$$

Where:

$$K1 = \frac{F_{passenger}}{\text{force threshold}} = \frac{M_s * \ddot{x}_s}{\text{force threshold}}$$

K1: is a variable gain that is used to give a priority to the control force when the force transmitted to the passenger $F_{passenger}$ increases. Therefore, the priority is to control the force by increasing the control signal of the force controller. The force controller responds directly to the force change and reacts to keep the forces within their limits. The force threshold is chosen in such a way as to keep the transmitted force, the position of sprung mass and the control signal within acceptable limits.

Increasing the threshold generates an increase in the position of sprung mass and the transmitted force.

Using high values for the threshold yields an unstable oscillatory performance.

We use two pass filters $\frac{\alpha_1}{s + \alpha_2}$ $\frac{\alpha_3}{s + \alpha_4}$ in order to accomplish a smooth merging of two controllers and to prevent the singularity that can occur in such highly nonlinear systems.

α_1 , α_3 are gains of the low pass filter that give priority to the corresponding filter.

α_2 , α_4 are designed to select the bandwidth.

Increasing these parameters to high values could generate instability in the system response.

The bandwidth of the filters should be also greater than the bandwidth of the active suspension system in order to accomplish full control of a wide range of the system's bandwidth (Wright 1983).
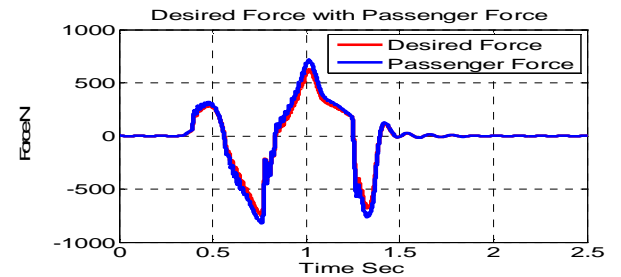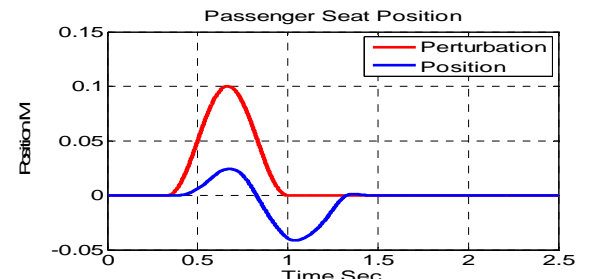

Figure 8: Force Tracking.
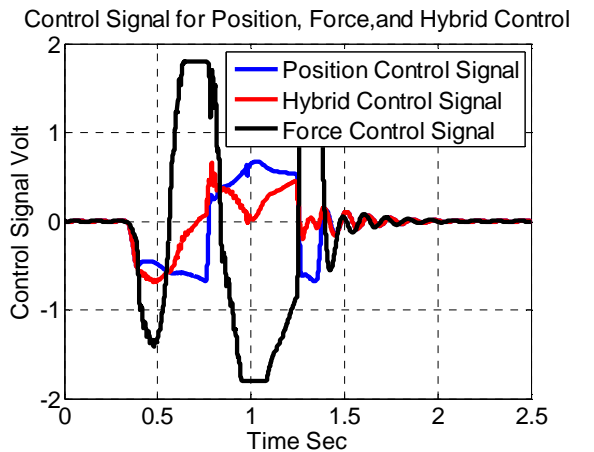

Figure 9: Sprung Mass Position.
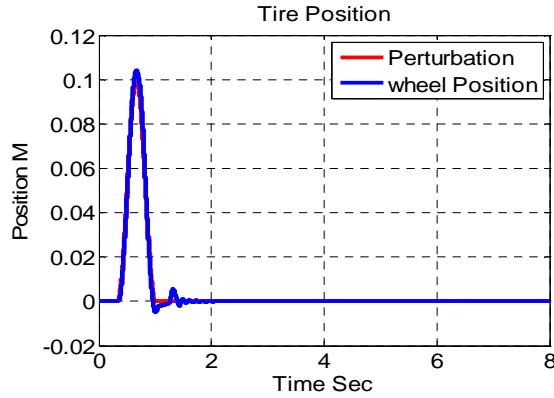

Figure 10: Control Signal

Figure 11: Unsprung Position

Figure 8 shows that the force transmitted to the passenger is limited to 717 N, with a small tracking error. The hybrid control also reduced the perturbation from 10 cm to 4.5 cm, which is another good index of controller robustness and performance as illustrated in Figure 9.

The control signal reaches a maximum of 0.6 volts, as seen in Figure 10. The road holding is proven to be good, as seen in Figure 11, in which the tire is attached to the road along with the perturbations.

6. COMPARISON OF THE CONVENTIONAL PID CONTROLLER WITH THE HYBRID SMC CONTROLLER

We will use a conventional PID for controlling the position of the sprung mass, and compare it with our proposed hybrid SMC. We chose the PID control because it is the most popular controller in the industry. The simulation results show that our proposed hybrid SMC exceeds the performance of the PID by a significant margin. The PID was designed using NCD Toolbox Simulink to produce optimal gains. We began by linearizing the nonlinear model, which gives us:

$$A = \begin{Bmatrix} 0 & 1 & 0 & 0 & 0 & 0 \\ -a_0 & -b_0 & a_0 & b_0 & a_1 & 0 \\ 0 & 0 & 0 & 1 & 0 & 0 \\ d_0 & d_1 & -d_0-h_1 & -d_1-b_1 & -c_1 & 0 \\ 0 & -J_1A & 0 & J_1A & -J_1L & -J_1c_d\,(P_s/\rho)^{1/2} \\ 0 & 0 & 0 & 0 & 0 & -1/\tau \end{Bmatrix},$$

$$B = \begin{vmatrix} 0 \\ 0 \\ 0 \\ 0 \\ 0 \\ K_v/\tau \end{vmatrix}, C = |1\ \ 0\ \ 0\ 0\ \ 0\ \ 0|, D = |\ 0|.$$

The PID gains are then applied to the nonlinear model. The results of the simulation show that the passenger's vertical motion has been reduced to zero faster and with smaller amplitude by the hybrid SMC controller than the PID (Figure 12). The transmitted force to a passenger with the PID has a longer settling time than with the SMC, and that is not very comfortable (Figure 13). In terms of the force

amplitude, the hybrid SMC produces a smaller controlled force in comparison with the PID due to the force controller, which acts on behalf of the position at that stage.
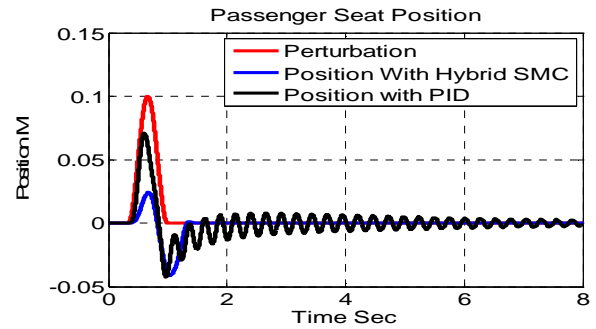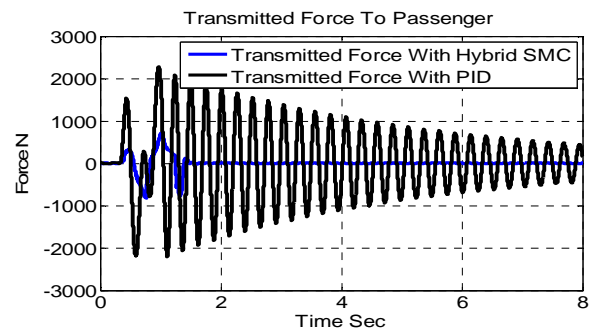

Figure 12: Sprung Mass Position

Figure 13: Transmitted Force to Passenger

7. CONCLUSION

This paper presents a force/position control for an active suspension system. Position control was achieved using the SMC controller, and the perturbations were reduced enough, but the force transmitted to the passenger was not acceptable. The resulting control signal has a slight chattering in simulation, but it is still within the acceptable limit. For reducing the transmitted force to the passenger, a force controller was developed to achieve good force tracking, but it did not produce a significant improvement with respect to the passenger seat position. In terms of force tracking, the desired force was derived from a desired acceleration. The hybrid force/position controller was developed and applied. Good force tracking was achieved with an attenuation of the vertical seat perturbations. Using this hybrid controller, the passenger seat was isolated from road irregularities with good road holding. The control signal that was produced has a combined form in order to fit the requirements. In this project, two objectives were achieved with a hybrid controller by integrating the advantages of each controller (position, force) and applying them to the system. In a future project, an application of our integrated controller in real time will be tested and applied to the active suspension bench in order to verify the validity of the proposed controller.

APPENDIX

A. Active suspension parameters

P_1, P_2	Pressure at cylinder's chambers	$P_s = P_1 + P_2$
β	Effective bulk modulus	7.995e8 N/m^2
L	Coefficient of total leakage due to pressure	9.047e-13 m^5/Ns
A	Piston area	3.35e-4 m^2
P_L	Load pressure	$P_2 - P_1$
P_S	Supply pressure	103.4e5 N/m^2
ρ	Hydraulic fluid density	867kg/m3
V_0	Actuator volume in one actuator chamber	135.4e-6 m^3
C_d	Flow discharge coefficient	0.63
M_u	Unsprung mass	59 kg
M_s	Actuator mass	290 kg
k_r	Tire spring stiffness	190,000 N/m
k_p	Load spring stiffness	16,812 N/m
B_r	Tire viscous damping	800 Ns/m
B_p	Load viscous damping	800 Ns/m
τ	Servo-valve time constant	0.01s

B. Controllers Parameters.

Position Control Parameters		
C_1	Gains sliding surface	125000
C_2	Gains sliding surface	7500
C_3	Gains sliding surface	150
C_4	Gains sliding surface	1
a	Sigmoid function	2000
K_{sw}	Switching gain	330000
Force Control Parameters		
C_1	Gains sliding surface	10000
PID Control Parameters		
K_p	Proportional gain	5
K_i	Integral gain	0.4
K_i	Derivative gain	0.1

C. Systems variables

x_r	External unknown perturbation	
$\dot{x}_r$	Speed of perturbation signal	
$x_1 = x_s$	Vertical position of the car body	
$\dot{x}_s$	Piston speed	
$x_2 = \dot{x}_1$	Vertical speed of the car body	
$x_3 = x_u$	Vertical position of the car wheel	
$x_4 = \dot{x}_3$	Vertical speed of the car wheel	
$x_5 = P_L$	Pressure difference in the circuit	
$x_6 = x_v$	Area of the servo valve orifice	
U	Control signal	

REFERENCES

Angue-Mintsa, H., Venugopal, R., et Kenne, J. P., and Belleau, C. 2011. Adaptive Position Control of an Electrohydraulic Servo System with Load Disturbance Rejection and Friction Compensation. *Journal of Dynamic Systems, Measurement, and Control* 133(6), 064506-1 - 064506-8

Assadsangabi, B., Eghtesad, M., Daneshmand, F., *and Vahdati, N., 2009. Hybrid sliding mode control of semi-active suspension* systems. *Smart Materials and Structures* 18(12), 1-10.

Avila, M. A., Loukianov, A. G.,and Peter D.L., 2004. Electro-hydraulic actuator trajectory tracking. *Proceedings of the American Control Conference*, pp.2603-2608, June 2004, Boston, USA.

Chantranuwathana, S. and Peng, H. 1999. Force tracking control for active suspensions – theory and experiments. *Proceedings of the IEEE International Conference on* Control Applications, pp. 442-447. August 22-27, Hawai'I, USA.

Chantranuwathana, S. and Peng, H, 2000. Practical adaptive robust controllers for active suspensions. *Proceedings of the 2000 ASME International Congress and Exposition*, Orlando,Florida, USA.

Choi, J. 2011 .Robust control of hydraulic actuator using back-stepping sliding mode controller. *Proceedings of the 28th ISARC,* pp. 1261-1266, Jun 29- Jul 2, Seoul, Korea.

Fallaha, C. J., Saad, M., Kanaan, H. Y., and Al-Haddad, K. 2011.Sliding-mode robot control with exponential reaching law. *IEEE Transactions on Industrial Electronics* 2011, 58(2), 600-610.

Hashemipour, H., Amiri, M. Mirzaei, M., and Maghoul, A., 2009. Nonlinear control of vehicle active suspension considering actuator dynamics. *Second International Conference on Computer and Electrical Engineering,* pp. 362-366. December 28-30. Dubai, UAE.

Indrawanto, T., Nurprasetio, P., Bagiasna, K., Suharto, D., Tjahjowidodo, T., Nik,W,W., Ahmad,A., Sulaiman,O., Syahrullail,S., 2011.Sliding Mode Control of a Single Rigid Hydraulically Actuated Manipulator. *International Journal of Mechanical and Mechatronics Engineering*, 11(5), 19-25.

Kaddissi, C., Saad, M., Kenne, Jean-Pierre., 2009. Interlaced backstepping and integrator forwarding for nonlinear control of an electrohydraulic active suspension. *Journal of Vibration and Control* 15(1), 101-131.

Merritt, H. E. 1967. Hydraulic control systems, Wiley, New York.

Nguyen, H, Q., Ha, Q, P,. Rye, D, C.,Durrant-whytel, H, F,. 2000. Force/position tracking for electrohydraulic systems of a robotic excavator. Decision and Control, 2000. *Proceedings of the 39th IEEE Conference,* pp. 5224-5229.December Sydney, Australia

Priyandoko, G., Mailah, M., and Jamaluddin, H., 2009. Vehicle active suspension system using skyhook adaptive neuro active force control. *Mechanical Systems and Signal Processing*, 23(3), 855-868.

Rahmat, M,F., Zulfatman, A,R., and Husain, K. I., Sam, Y. M., Ghazali, R., and Rozali, S. M., 2011. Modeling and controller design of an industrial hydraulic actuator system in the presence of friction and internal leakage. *International Journal of the Physical Sciences,* 6(14), 3502-3517.

Sam, Y. M. and Hudha, K., 2006. Modelling and force tracking control of hydraulic actuator for an active suspension system. *First IEEE Conference on Industrial Electronics and Applications*, pp.24-26 May 2006, Piscataway, NJ, USA.

Shi, M., Liu, X., and Shi, y.,2011. Research on enhanced ADRC algorithm for hydraulic active suspension. *Proceedings of the International IEEE Conference on Transportation, Mechanical, and Electrical Engineering*, pp. 1539-1543. December 16-18, Changchun, China.

Sohl, G. A., Bobrow, J. E. 1999. Experiments and simulations on the nonlinear control of a hydraulic servosystem. ,*IEEE Transactions on Control Systems Technology*, 7(2), 238-247.

Tafazoli, S., Clarence, S., and Peter, L., 1998. Tracking control of an electrohydraulic manipulator in the presence of friction. *IEEE Transactions on Control Systems Technology*, 6(3), 401-411.

Wright, P. G., 1983. The influence of aerodynamics on the design of Formula One racing cars. *International Journal of Vehicle Design*, 3(4), 383-397.